Articles

A Model-Independent, Nonlinear Extrapolation Procedure for the Characterization of Protein Folding Energetics from Solvent-Denaturation Data[†,‡]

Beatriz Ibarra-Molero and Jose M. Sanchez-Ruiz*

Departamento de Quimica Fisica (Facultad de Ciencias), Instituto de Biotecnologia, 18071-Granada, Spain

Received July 24, 1996; Revised Manuscript Received September 20, 1996[⊗]

ABSTRACT: We have characterized the guanidine-induced denaturation of hen egg white lysozyme within the 30−75 °C temperature range on the basis of equilibrium fluorescence measurements, unfolding assays, kinetic fluorescence measurements, and differential scanning calorimetry. Analysis of the guanidine denaturation profiles according to the linear extrapolation method yields values for the denaturation Gibbs energy which are about 15 kJ/mol lower than those derived from differential scanning calorimetry. Our results strongly suggest that this discrepancy is not due to deviations from the two-state denaturation mechanism. We propose a new method for the determination of denaturation Gibbs energies from solvent-denaturation data (the constant-ΔG extrapolation procedure). It employs several solvent-denaturation profiles (obtained at different temperatures) to generate the protein stability curve at zero denaturant concentration within the −8 to 8 kJ/mol ΔG range. The method is model-independent and provides a practical, nonlinear alternative to the commonly employed linear extrapolation procedure. The application of the constant-ΔG method to our data suggests that the guanidine-concentration dependence of the denaturation Gibbs energy is approximately linear over an extended concentration range but, also, that strong deviations from linearity may occur at low guanidine concentrations. We tentatively attribute these deviations to the abrupt change of the contribution to protein stability that arises from pairwise charge−charge electrostatic interactions. This contribution may be positive, negative, or close to zero, depending on the pH value and the charge distribution on the native protein surface [Yang, A.-S., & Honig, B. (1993) *J. Mol. Biol. 231,* 459−474], which may help to explain why disparate effects have been found when studying protein denaturation at low guanidine concentrations. Kinetic *m* values for lysozyme denaturation depend on temperature, in a manner which appears consistent with Hammond behavior.

Many fundamental studies on protein folding rely heavily on denaturation Gibbs energy values derived from experimental data. Differential scanning calorimetry (DSC)[1] is unsurpassed in its capability to provide a detailed energetic description of protein reversible denaturation (Sturtevant, 1987; Privalov, 1989; Freire, 1995; Sanchez-Ruiz, 1995; Makhatadze & Privalov, 1995). Nevertheless, denaturation Gibbs energies are very often determined from experimental studies on urea- or guanidine-induced denaturation. Some of the reasons for this are (1) solvent-denaturation experiments are fast and simple, while calorimetric instrumentation may not be available in some laboratories; (2) irreversibility is often found in thermal denaturation of proteins and, in many cases, precludes the equilibrium thermodynamics analysis of DSC thermograms (Sanchez-Ruiz, 1992, 1995); on the other hand, some of the processes responsible for the irreversibility (aggregation) are less likely to occur in denaturing concentrations of urea or guanidine; (3) when based on fluorescence measurements, solvent-denaturation studies may be carried with protein concentrations in the range of micromolar, which is convenient for work with valuable samples and further disfavors aggregation.

The main drawback of the solvent-denaturation method is that extra-thermodynamic assumptions must be employed in the data analysis. Thus, besides the presupposition of two-state behavior, the dependence of the denaturation Gibbs energy with denaturant concentration is usually assumed to be linear *outside* the transition zone. The validity of this *linear extrapolation approximation* has been discussed from both the theoretical (Schellman, 1978, 1987; Alonso & Dill, 1991) and experimental (Pace & Vanderburg, 1979; Santoro & Bolen, 1988, 1992; Bolen & Santoro, 1988; Hu et al., 1992; Ahmad et al., 1994; Johnson & Fersht, 1995; Yao & Bolen, 1995) points of view. However, no clear conclusion has emerged yet. Thus, in two cases in which the denaturation Gibbs energy was determined over a wide denaturant-concentration range (from DSC experiments carried out at different denaturant concentrations), clear deviations from linearity were found (Santoro & Bolen, 1992; Johnson & Fersht, 1995). On the other hand, Myers et al. (1995) have pointed out that in most studies of protein denaturation at

[†] This research was supported by Grant PB93-1087 from the DGICYT (Spanish Ministry of Science and Education). B.I.-M. is a recipient of a predoctoral fellowship from the Spanish Ministry of Science and Education.

[‡] This paper is dedicated to the memory of Dolores Molero.

[⊗] Abstract published in *Advance ACS Abstracts,* November 1, 1996.

[1] Abbreviations: DSC, differential scanning calorimetry; HEW, hen egg white.

S0006-2960(96)01836-3 CCC: $12.00

low denaturant concentrations no deviations from linearity are observed (see Discussion section in Myers et al. and references quoted therein). An excellent discussion on the asumptions involved in the linear extrapolation method may be found in Yao and Bolen (1995).

Regardless of its (uncertain) validity, the widespread use of the linear extrapolation method is to be attributed to the fact that there appears to be no practical alternatives. Of course, nonlinear methods are known, but they are based on simplified models and usually require that the values of additional parameters be assumed, thus adding uncertainty to the calculated denaturation Gibbs energies. For instance, application of the denaturant binding model (Aune & Tanford, 1969) requires the assumption of a value for the equilibrium binding constant.

The main purpose of the present work is to introduce a new extrapolating method which shows the following features. (1) It does not assume a linear dependence of the denaturation Gibbs energy with denaturant concentration. (2) It is model-independent. (3) All parameters involved in the method are determined from the experimental solvent-denaturation data. The method (named the constant-ΔG extrapolation procedure) will be tested with published data for the urea-induced denaturation of barnase (Johnson & Fersht, 1995) and with experimental data reported in the present work on the guanidine-induced denaturation of lysozyme [as will be demonstrated here, the linear extrapolation estimates of the Gibbs energy change for lysozyme denaturation differ from the actual values (as calculated from DSC experiments) by a large energy amount, about 15 kJ/mol]. We also believe that the analyses reported in this work shed some light on the nature of electrostatic contributions to protein stability. Finally, we conclude this introduction by giving some basic theoretical results which will be used throughout this work:

At constant temperature, the effect of denaturant concentration (C) on denaturation Gibbs energy (ΔG) can always be expressed as a Taylor expansion around the concentration ($C_{1/2}$) at which $\Delta G = 0$:

$$\Delta G = \left(\frac{\partial \Delta G}{\partial C}\right)_{C_{1/2}} \times (C - C_{1/2}) + \frac{1}{2}\left(\frac{\partial^2 \Delta G}{\partial C^2}\right)_{C_{1/2}} \times (C - C_{1/2})^2 + \ldots \quad (1)$$

where all derivatives are evaluated at $C_{1/2}$. Experiments, however, only yield reliable ΔG data in a narrow concentration range around $C_{1/2}$ (the transition zone); as a result, the data do not contain information about higher-order terms in eq 1, and within that narrow range, they are adequately represented by the expansion truncated in the linear term:

$$\Delta G \cong -m_{1/2}(C - C_{1/2}) \quad (2)$$

where $m_{1/2}$ stands for minus the derivative $(\partial \Delta G/\partial C)$ *evaluated at* $C_{1/2}$. Substituting $C = 0$ in eq 2 we obtain the "linear extrapolation" estimate for the denaturation Gibbs energy in water (at zero denaturant concentration):

$$\Delta G_W = m_{1/2} \cdot C_{1/2} \quad (3)$$

and substituing back in eq 2 we arrive at the familiar expression

$$\Delta G = \Delta G_W - m_{1/2} \cdot C \quad (4)$$

Equation 1 (with infinite terms in the expansion) is completely general but useless. Equation 2 provides an adequate representation of the ΔG data *within* the narrow transition zone. Equations 3 and 4 may be used to calculate the denaturation Gibbs energy at zero denaturant concentration (they, of course, will yield the same value for ΔG_W); this calculation, however, assumes that the dependence of ΔG with C is linear *outside* the transition zone.

MATERIALS, METHODS, AND EXPERIMENTAL DATA ANALYSIS

Materials. Hen egg white (HEW) lysozyme was purchased from Sigma Chemical Co. Guanidinium hydrochloride was ultrapure grade from Pierce. Both were used without further purification. Deionized and degassified water was used throughout. Aqueous stock solutions of lysozyme were prepared by exhaustive dialysis against sodium acetate (50 mM, pH 4.5). Protein concentrations were determined spectrophotometrically, using a published value for the extinction coefficient at 280 nm (Canfield, 1963). Stock solutions of guanidinium hydrochloride (usually at concentrations about 8 M) were prepared by dissolving the solid product in a dialysis buffer that had been equilibrated with the protein solution. Lysozyme solutions in water−guanidine were prepared by mixing the required volumes of the stocks solutions of lysozyme and guanidine. Guanidine concentrations were determined from refraction index measurements (Pace at al., 1989). The pH meter reading for lysozyme solutions in denaturing concentrations of guanidine was found to be 4.3−4.4, instead of 4.5 (the pH of the aqueous stock solution of lysozyme). No attempt was made, however, to adjust the pH meter reading to 4.5, given that pH meter readings in water−cosolvent mixtures must be subject to corrections in order to obtain the true pH values (Bates, 1973). To the best of our knowledge, the correction factors for the measurement of pH in water−guanidine have not been published. Of course, adjusting the pH meter reading of the lysozyme solutions in water−guanidine to 4.5 (by adding NaOH, for instance) does not guarantee that the pH value is 4.5. In any case, the pH dependence of the energetic parameters for lysozyme denaturation appears to be very small around pH 4.5 (Pfeil & Privalov, 1976), and a pH change of a few tenths is not expected to be of significant consequence. Note that, throughout the text, we refer nominally to the buffer conditions employed in this work as sodium acetate, pH 4.5.

Lysozyme Equilibrium Denaturation Studied by Steady-State Fluorescence Measurements. The fluorescence of the protein in guanidinium hydrochloride solutions was measured by using a Perkin-Elmer LS-5 instrument with excitation and emission wavelengths of 280 and 360 nm, respectively. Prior to the fluorescence measurements, the protein (concentration about 4 μM) had been kept in the denaturant solutions for a time sufficient to ensure that the denaturation equilibrium was established. Profiles of fluorescence intensity versus denaturant concentration were obtained at several temperatures within the range 30−56 °C (see Figure 1). These profiles were analyzed according to a two-state denaturation model:

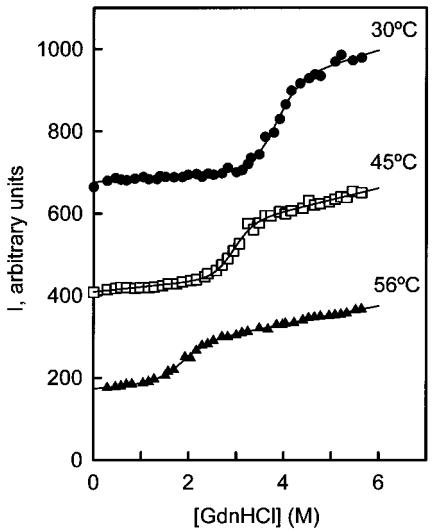

FIGURE 1: Examples of equilibrium profiles of lysozyme fluorescence intensity at 360 nm (excitation at 280 nm) versus guanidine concentration. The lines represent the best fits of eq 6 to the fluorescence intensity data.

$$I = I_N \cdot X_N + I_D \cdot X_D \quad (5)$$

where I is the measured fluorescence intensity, I_N and I_D are the fluorescence intensities for the native and denatured states, and X_N and X_D stand for the mole fractions of these states. Both I_N and I_D were assumed to depend linearly on denaturant concentration (C): $I_N = \alpha_N + \beta_N \cdot C$, $I_D = \alpha_D + \beta_D \cdot C$. Mole fractions are related with the denaturation equilibrium constant [$X_N = 1/(1 + K)$, $X_D = K/(1 + K)$], which is given by $K = \exp(-\Delta G/RT)$. Finally, using eq 2 for the denaturation Gibbs energy we arrive at:

$$I = \frac{(\alpha_N + \beta_N \cdot C) + (\alpha_D + \beta_D \cdot C)e^{m_{1/2}(C - C_{1/2})/RT}}{1 + e^{m_{1/2}(C - C_{1/2})/RT}} \quad (6)$$

The nonlinear, least-squares fittings of eq 6 to the experimental I versus C profiles were carried out by using the program MLAB (Civilized Software, Inc.). Fits were always excellent (see Figure 1). Note that eq 6 involves six fitting parameters: α_N, β_N, α_D, β_D, $C_{1/2}$, and $m_{1/2}$ (where α_N, β_N, α_D, and β_D describe the pre- and posttransition base lines). Linear extrapolation estimates of the denaturation Gibbs energy in water (ΔG_W) were calculated from the $C_{1/2}$ and $m_{1/2}$ values by using eq 3.

Lysozyme Equilibrium Denaturation Studied by Unfolding Assays. The mole fraction of protein present as native state under given solvent conditions (denaturant concentration, temperature) may be determined from the denaturation kinetics observed after transferring the protein to strongly unfolding conditions (unfolding assay). Under these conditions, intermediate (partially unfolded) states are expected to denature much faster than the native state does; thus, it is possible to monitor separately the denaturation of the native state and to calculate the amount of native state in the original solution from the amplitude of the observed exponential kinetics (Mücke & Schmid, 1994). In our unfolding assays, protein (concentration about 1 mg/mL), was incubated in guanidinium hydrochloride solutions at a given temperature for a time sufficient to ensure that denaturation equilibrium had been established, and subsequently, the unfolding kinetics were initiated by a 25-fold dilution into an unfolding buffer so that the following final conditions were obtained, denaturant concentration, 7.8 M, pH 4.5 (with 50 mM acetate buffer); temperature, 18 °C. Under these conditions, the half-life for native state denaturation is about 3 min. Denaturation kinetics were monitored by following the time dependence of the fluorescence emission at 360 nm with excitation at 280 nm. Fluorescence intensity versus time profiles gave excellent fits to the following first-order rate equation (see Figure 2A):

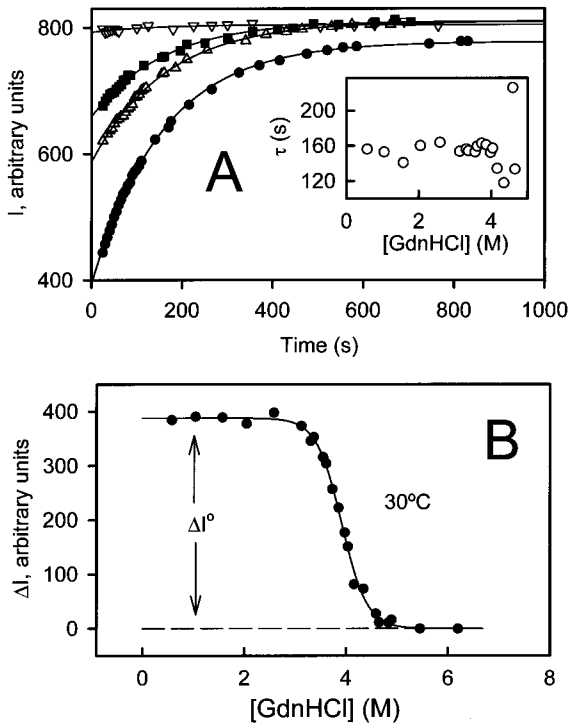

FIGURE 2: (A) Profiles of fluorescence intensity versus time recorded after transferring lysozyme (previously incubated at 30 °C in a given guanidinium hydrochloride solution until equilibrium had been established) to strongly unfolding conditions (7.8 M guanidine, pH 4.5, T = 18 °C). The guanidine concentrations in the initial solutions were (●) 0.58, (△) 3.85, (■) 4.04, and (▽) 4.65 M. The lines represent the best fits of eq 7 to the fluorescence intensity data, and the inset shows the half-life values derived from these fittings. The fact that τ remains essentially constant supports that the native molecules which are populated in the transition region (see panel B below) are indistinguishable from the native molecules as they exist under native conditions (Mücke & Schmid, 1994). (B) Unfolding amplitudes calculated from the fitting of eq 7 to unfolding kinetics such as those shown in panel A. These amplitudes are proportional to the amount of native protein in the initial solutions and are plotted versus the guanidine concentration in those solutions. The line represents the best fit of eq 8 to the unfolding amplitude data.

$$I = I_\infty - \Delta I \cdot e^{-t/\tau} \quad (7)$$

where I_∞ is the fluorescence intensity at $t = \infty$ and ΔI stands for the amplitude of the exponential, which is proportional to the mole fraction of the native state in the original denaturant solution: $\Delta I = \Delta I^0 \cdot X_N$. Profiles of ΔI versus denaturant concentration were obtained at several temperatures within the range 30−45 °C. Assuming a two-state model, ΔI may be expressed as:

$$\Delta I = \frac{\Delta I^0}{1 + e^{m_{1/2}(C - C_{1/2})/RT}} \quad (8)$$

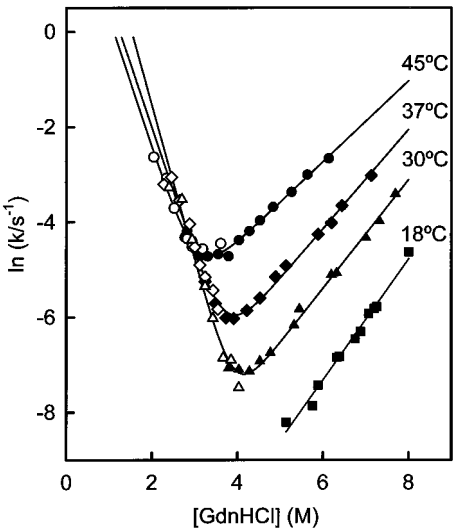

FIGURE 3: Chevron plots of folding−unfolding rate constant for lysozyme versus guanidine concentration for several temperatures. Empty and filled symbols correspond, respectively, to kinetic experiments performed in the folding and unfolding directions. The lines represent the best fits of the dependency predicted by eqs 9−11, except for $T = 18$ °C (a simplified form of the equations was used in this case; see text for details).

Nonlinear, least-squares fits of eq 8 to the experimental ΔI versus C profiles (using the program MLAB) were always excellent (see Figure 2B). Equation 8 involves three fitting parameters: ΔI^0, $m_{1/2}$, and $C_{1/2}$. Note that the value of ΔI^0 equals the value of ΔI calculated for denaturant concentrations clearly below the transition zone (see Figure 2B). Note also that, while eq 8 involves the two-state assumption, the calculation of the mole fraction of protein present as native state from $X_N = \Delta I/\Delta I^0$ *does not* (Mücke & Schmid, 1994).

Linear extrapolation estimates of the denaturation Gibbs energy in water (ΔG_W) were calculated from the $C_{1/2}$ and $m_{1/2}$ values by using eq 3.

Lysozyme Folding−Unfolding Kinetics Studied by Steady-State Fluorescence Measurements. Folding−unfolding kinetics were studied by following the time dependence of the protein fluorescence emission at 360 nm (excitation at 280 nm) after suitable denaturant-concentration jumps (20-fold dilution from 8 M guanidine or from zero denaturant concentration for experiments carried out at denaturant concentrations below or above $C_{1/2}$, respectively). Apparent folding−unfolding rate constants (k) were calculated from the fittings of a first-order rate equation ($I = I_\infty - \Delta I \cdot e^{-kt}$) to the experimental fluorescence intensity versus time data. These fits were always excellent. Figure 3 shows Chevron plots of ln k versus denaturant concentration obtained at several temperatures. These plots have been analyzed according to a two-state *kinetic* model:

$$\ln k = \ln(k_F + k_U) \tag{9}$$

where k_F and k_U are the folding and unfolding rate constants, respectively. The denaturant concentration dependencies of k_F and k_U are given by:

$$\ln k_F = \ln k_{1/2} + \frac{m_{U-\ddagger}}{RT}(C - C_{1/2}) \tag{10}$$

$$\ln k_U = \ln k_{1/2} + \frac{m_{N-\ddagger}}{RT}(C - C_{1/2}) \tag{11}$$

where $m_{U-\ddagger}$ and $m_{N-\ddagger}$ describe the denaturant-concentration effect on the activation Gibbs energies for folding and unfolding, respectively [$m_{U-\ddagger} = -(\partial \Delta G_{U-\ddagger}/\partial C)$, $m_{N-\ddagger} = -(\partial \Delta G_{N-\ddagger}/\partial C)$], and $k_{1/2}$ is the value of both k_F and k_U at $C = C_{1/2}$. Equations 10 and 11 assume that the activation Gibbs energies change linearly with denaturant concentration (that is, $m_{U-\ddagger}$ and $m_{N-\ddagger}$ are taken as constants) and can be easily derived from transition-state theory (Chen at al., 1992). The applicability of the two-state kinetic model and transition-state theory to lysozyme denaturation has been discussed and supported by Schmid (1992); see also Segawa and Sugihara (1984a,b).

The nonlinear, least-squares fittings (MLAB program) of the ln k versus C dependence predicted by eq 9, together with eqs 10 and 11, to the experimental profiles corresponding to 30, 37, and 45 °C were excellent (Figure 3). Equations 9−11 contain four fitting parameters: $C_{1/2}$, $k_{1/2}$, $m_{U-\ddagger}$ and $m_{N-\ddagger}$. Nevertheless, the equilibrium $m_{1/2}$ value may be calculated from the kinetic m values by using:

$$m_{1/2} = m_{N-\ddagger} - m_{U-\ddagger} \tag{12}$$

and again, the linear extrapolation estimate of the denaturation Gibbs energy in water may be obtained from this $m_{1/2}$ value and that of $C_{1/2}$ by using eq 3.

For $T = 18$ °C we only characterized the unfolding branch of the Chevron plot (Figure 3). These data were fitted with the equation $\ln k_U = \ln k_0 + m_{N-\ddagger} \cdot C/RT$, where k_0 is the linear extrapolation estimate of the unfolding rate constant for $C = 0$.

Calculation of the Protein Stability Curve for Lysozyme at Zero Denaturant Concentration from Differential Scanning Calorimetry Data. The thermal denaturation of lysozyme has been previously studied by high-sensitivity differential scanning calorimetry (Pfeil & Privalov, 1976; Privalov, 1979; Makhatadze & Privalov, 1993; Privalov & Makhatadze, 1993), and the temperature dependencies of the denaturational changes in enthalpy and heat capacity are accurately known; see data collected in the recent review by Makhatadze and Privalov (1995). In fact, these reported ΔH and ΔC_p data should apply to our solvent conditions (in the absence of denaturant), since we used a buffer with a negligible ionization heat. On the other hand, the denaturation temperature of a protein (T_m) is very sensitive to solvent conditions. Accordingly, we determined the T_m value under our solvent conditions from DSC experiments carried out in a calorimeter DASM-1 described by Privalov et al. (1975), with cell volumes of 1 mL, under an extrapressure of 1 atm to avoid any degassing during the heating. Most experiments were performed at a scanning rate of 1.76 K/min; however, additional experiments at lower scanning rates gave essentially identical results. A single transition was always observed in the DSC thermograms. Analysis of these DSC transitions was carried out as described previously (Sanchez-Ruiz, 1995; Plaza del Pino & Sanchez-Ruiz, 1995).

The protein stability curve (the ΔG_W versus temperature profile) for lysozyme in water (pH 4.5, 50 mM sodium acetate) was calculated by numerical integration of the Gibbs−Helmholtz equation:

$$\Delta G_W = -T\int_{T_m}^{T} \frac{\Delta H}{T^2} dT \tag{13}$$

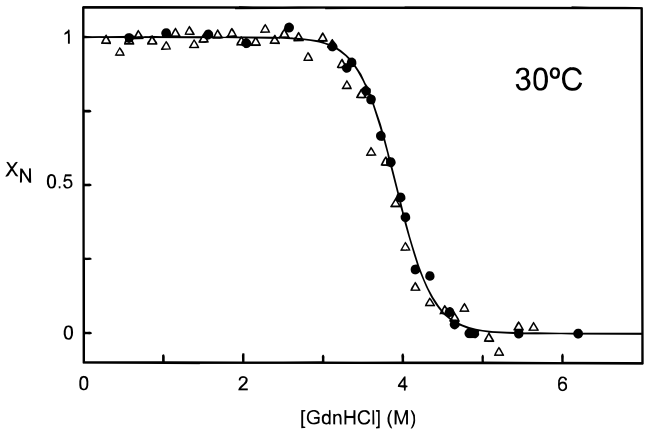

FIGURE 4: Equilibrium profile of mole fraction of native protein versus guanidine concentration for lysozyme at 30 °C: (△) values calculated from fluorescence intensity data (Figure 1), together with the denaturant-concentration dependencies of the fluorescence intensities for the native and denatured states, as determined from the fitting of eq 6 to the fluorescence intensity data (Figure 1), and (●) values derived from unfolding assays and calculated as $\Delta I/\Delta I^0$. It should be noted that the calculation of the mole fraction of the native state in this manner does **not** involve the two-state assumption (Mücke & Schmid, 1994). The continuous line is the dependence predicted by the $C_{1/2}$ and $m_{1/2}$ values derived from the analysis (by using eqs 9−11) of the Chevron plots shown in Figure 3.

The T_m value used was that corresponding to the solvent conditions employed in this work (calculated from our DSC experiments); ΔH values as a function of temperature were interpolated from the data given by Makhatadze and Privalov (1995); these data show a nonlinear dependence of ΔH with temperature, reflecting the fact that, strictly, ΔC_p is not temperature-independent.

We believe that the above calculation, which combines the T_m value determined for the buffer and pH conditions employed in this work with accurate enthalpy reported in the literature and which takes into account the temperature dependence of the ΔC_p value, provides the most reliable protein stability curve we can calculate for lysozyme denaturation in water, pH 4.5, 50 mM sodium acetate (see Figures 5 and 9). We note, nevertheless, that a simpler calculation assuming that ΔC_p does not depend on temperature:

$$\Delta G_W = \Delta H_m\left(1 - \frac{T}{T_m}\right) + \Delta C_p\left[T - T_m - T\ln\left(\frac{T}{T_m}\right)\right] \quad (14)$$

and using the ΔH_m (denaturation enthalpy at the denaturation temperature) and ΔC_p values derived from *our* calorimetric experiments yields very similar results (thus, within the temperature range considered in this work, the two protein stability curves differ by less than 2 kJ/mol; see Figures 5 and 9).

Calculation of the Denaturant $m_{1/2}$ Value for Lysozyme Denaturation from Differential Scanning Calorimetry Data. Denaturant $m_{1/2}$ values may be calculated from the denaturant concentration effect on the parameters derived from the DSC transitions. The effect of denaturant concentration on the denaturation temperature may be expressed as:

$$(dT_m/dC) = (\partial T/\partial C)_{\Delta G=0} = -\frac{(\partial \Delta G/\partial C)_T}{(\partial \Delta G/\partial T)_C} = -\frac{m_{1/2}}{\Delta S_m} \quad (15)$$

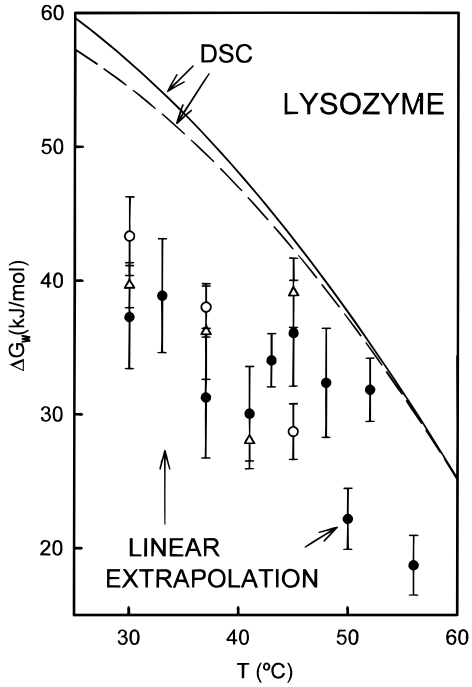

FIGURE 5: Temperature dependence of the Gibbs energy change for lysozyme denaturation at zero denaturant concentration (sodium acetate, pH 4.5). Linear extrapolation estimates were obtained from the analysis of three different types of experimental data for guanidine-induced denaturation: (●) profiles of fluorescence intensity versus guanidine concentration (Figure 1), (△) profiles of unfolding amplitude versus guanidine concentration (Figure 2), and (○) profiles of folding−unfolding rate constant versus guanidine concentration (Chevron plots of Figure 3). Error bars represent the associated standard errors, as given by the MLAB program. The lines are the protein stability curves derived from DSC data. Continuous line: stability curve calculated from the T_m value (76.9 °C) corresponding to the solvent conditions employed in this work (50 mM sodium acetate, pH 4.5), together with the denaturation enthalpies given by Makhatadze and Privalov (1995); this calculation (eq 13) takes into account the temperature dependence of the denaturation heat capacity. Dashed line: stability curve calculated from the T_m, ΔH_m, and ΔC_p values (76.9 °C, 583 kJ·mol^{-1}, and 7.2 kJ·K^{-1}·mol^{-1}, respectively) derived from DSC experiments under the solvent conditions employed in this work, assuming that ΔC_p does not change with temperature (eq 14).

where ΔS_m is the denaturation entropy at the T_m value corresponding to a given denaturant concentration. In eq 15 we have first used that $\Delta G = 0$ for $T = T_m$, then we have employed some known mathematical properties of partial differentiation (Blinder, 1966), and finally, we have taken into account the definitions of $m_{1/2}$ and ΔS as partial derivatives of ΔG. Since $\Delta S_m = \Delta H_m/T_m$, we arrive at the following expression for $m_{1/2}$:

$$m_{1/2} = -\frac{\Delta H_m}{T_m}\left(\frac{dT_m}{dC}\right) \quad (16)$$

which allows us to calculate $m_{1/2}$ from the values of the denaturation enthalpy and denaturation temperature obtained from several DSC experiments carried out at different denaturant concentrations. Accordingly, we performed calorimetric experiments at four denaturant concentrations within the range 0−0.52 M. The slope dT_m/dC in eq 16 was estimated from a linear fit of T_m versus C, and the calculated $m_{1/2}$ values are shown in Figure 6. We have also applied this procedure to the calorimetric data reported by Privalov and Makhatadze (1992) on lysozyme denaturation

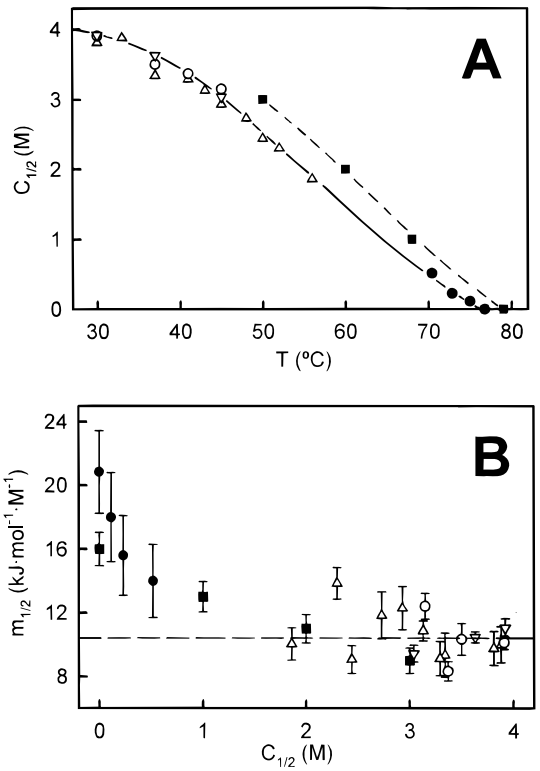

FIGURE 6: (A) Guanidine concentration−temperature equilibrium line for lysozyme: (○, △, ▽, ●) values obtained in this work from four different types of experimental data for guanidine-induced denaturation; (△) equilibrium fluorescence intensity data (Figure 1 and eq 6), (○) unfolding assays (Figure 2 and eq 8), (▽) folding−unfolding rate constants (Figure 3 and eqs 9−11), and (●) DSC experiments carried out at several guanidine concentrations (eq 16). The data represented by black squares are taken from the DSC study of Makhatadze and Privalov (1992); solvent conditions employed by these authors are slightly different from those employed in this work, and their data define an equilibrium line (dashed line) which is slightly above that defined by our data (continuous line). The lines are shown to guide the eye and have no theoretical meaning. (B) Denaturant $m_{1/2}$ for lysozyme denaturation calculated from the four types of experimental data described in panel A (the meaning of the symbols is the same as in panel A). Note that values derived from DSC data (eq 16) are represented by filled symbols. Bars represent the associated standard errors given by the MLAB program or, in the case of the values derived from DSC data, derived by linear propagation error assuming a typical error of 15 kJ/mol for the denaturation enthalpy in eq 16. The dashed line represents the average $m_{1/2}$ value calculated from the values within the 1.8−4 M range ($\langle m_{1/2} \rangle = 10.5$ kJ·mol^{-1}·M^{-1}).

in guanidinium hydrochloride solutions. These data were obtained under buffer and pH conditions somewhat different from those employed in this work; nevertheless, the $m_{1/2}$ values derived from them show a good agreement with those calculated from our data (Figure 6).

RESULTS AND DISCUSSION

Comparison between the Linear Extrapolation Estimates of the Gibbs Energy Change for Lysozyme Denaturation and the Protein Stability Curve Derived from Differential Scanning Calorimetry Experiments. We have calculated linear extrapolation estimates of the Gibbs energy change for lysozyme denaturation in water, within the temperature range 30−56 °C, from the analysis of three different types of experimental data for guanidine-induced denaturation. (1) Profiles of fluorescence intensity versus denaturant concentration (Figure 1)—these were analyzed according to a two-state equilibrium model (eq 6). (2) Amplitudes of the exponential denaturation kinetics observed after transferring the protein (previously incubated in a given guanidinium hydrochloride solution) to strongly unfolding conditions (unfolding assays)—these amplitudes should be proportional to the amount of native state present in the starting solution; profiles of unfolding amplitude versus denaturant concentration (Figure 2B) were also analyzed according to a two-state equilibrium model (eq 8). (3) Profiles of apparent folding−unfolding rate constant versus denaturant concentration (Chevron plots, see Figure 3)—these profiles were analyzed according to a two-state *kinetic* model (eqs 9−11); this analysis yields values for kinetic *m* values, which can be combined (eq 12) to produce the equilibrium $m_{1/2}$ value required for the linear extrapolation calculation of ΔG_W.

There is an excellent agreement (Figure 5) between the linear extrapolation estimates of ΔG_W calculated by using the three procedures described above. However, the calculated ΔG_W values are significantly lower (by about 15 kJ/mol) than the protein stability curve derived from DSC data (eqs 13 and 14). The discrepancy could hardly be attributed to the presence of intermediate states significantly populated during the guanidine-induced denaturation (that is, to a breakdown of the two-state assumption employed in the data analysis). Thus, Figure 4 shows profiles of mole fraction of native protein (X_N) versus denaturant concentration calculated from the three different types of experimental measurements described above; the agreement is excellent. It is very important to note that the calculation of X_N from unfolding assays does **not** involve the two-state assumption, that is, the ratio $\Delta I/\Delta I^0$ (see Materials, Methods, and Experimental Data Analysis) yields the mole fraction of native protein, even if intermediate states are significantly populated. Therefore, the agreement found between the X_N versus *C* profiles calculated from the two-state analysis of fluorescence data and Chevron plots with the X_N data calculated from unfolding assays (Figure 4) strongly supports that the two-state mechanism holds in this case. The fact that values of the mole fraction of native protein derived from unfolding assays may provide a two-state test for solvent-induced denaturation has been convincingly put forward by Mücke and Schmid (1994).

Change of the Equilibrium $m_{1/2}$ Value for Lysozyme Denaturation Along the Denaturant-Concentration−Temperature Equilibrium Line. We have determined equilibrium $m_{1/2}$ values for guanidine-induced denaturation of lysozyme from the analysis of four different types of experimental data: (1) profiles of fluorescence intensity versus denaturant concentration (Figure 1), (2) profiles of unfolding amplitude versus denaturant concentration (Figure 2), where the unfolding amplitudes were obtained from unfolding assays (see Materials, Methods, and Experimental Data Analysis) and are proportional to the mole fraction of native protein, (3) profiles of apparent folding−unfolding rate constant versus denaturant concentration (Chevron plots, Figure 3) and (4) effect of denaturant concentration on the parameters (denaturation temperature and denaturation enthalpy) obtained from the analysis of DSC thermograms for lysozyme denaturation (eq 16). There is a good agreement between the $m_{1/2}$ values obtained by using these four procedures (Figure 6B).

It should be noted at this point that the analysis of experimental profiles for guanidine-induced denaturation at

constant temperature yields (among other parameters) the values of $C_{1/2}$ for given temperatures, while DSC thermograms for the thermal denaturation of the protein in the presence of constant denaturant concentrations yield (among other parameters) the denaturation temperature (T_m) for given denaturant concentrations. However, regardless of the employed terminology ($C_{1/2}$ for given T or T_m for given C), in both cases the analyses of the experimental data provide couples of temperature−denaturant concentration for which the denaturation Gibbs enegy is zero. In other words, they provide points belonging to the equilibrium, denaturant-concentration−temperature line (that is, the $\Delta G = 0$, $C-T$ line). This $C-T$ equilibrium line for lysozyme denaturation is shown in Figure 6A. The values calculated for $m_{1/2}$ correspond to this line, that is, each calculated $m_{1/2}$ value is assigned to a couple temperature−denaturant concentration for which $\Delta G = 0$. Thus, the plot of $m_{1/2}$ *verus* $C_{1/2}$ shown in Figure 6B suggests that $m_{1/2}$ remains roughly constant (around 10−11 kJ·mol^{-1}·M^{-1}) at high denaturant concentration and increases sharply (up to 16−20 kJ·mol^{-1}·M^{-1}) below 1 M guanidine, but strictly speaking, we cannot rule out the possibility that the observed change is due to a temperature effect (since both C and T change simultaneously along the equilibrium line).

Constant-ΔG Extrapolation Procedure. Only denaturation Gibbs energy values within a narrow range around the zero value may be accurately determined from the analysis of solvent-denaturation data. We conservatively estimate this range as spanning from −8 to 8 kJ/mol, which corrresponds to a range of mole fraction of native state from about 0.95 to about 0.05, that is, for ΔG values higher than −8 kJ/mol and lower than 8 kJ/mol, both the native and denatured states may be said to be significantly populated. Within the narrow −8 to 8 kJ/mol range, the denaturant-concentration dependence of ΔG is adequately described by a linear expression (eq 2). However, we seek to obtain values for the denaturation Gibbs energy in water, which, *at room temperature*, are usually much higher than the upper limit of the "reliable" range (see, for instance, Figure 5). If a single solvent-induced denaturation profile (at a given temperature) has been obtained, the only feasible, model-free approach to calculate ΔG_W is the linear extrapolation method, that is, the use of eq 2 outside the −8 to 8 kJ/mol range.

On the other hand, if several denaturation profiles at several temperatures are available, then an alternative model-free approach exists. Instead of carrying out a denaturant-concentration extrapolation at constant temperature, we simultaneously change C and T along the extrapolation in such a way that ΔG remains constant and equal to a previously chosen value, ΔG^*, within the −8 to 8 kJ/mol range. More specifically, for a given temperature, T^*, at which the solvent-denaturation profile and the $C_{1/2}$ and $m_{1/2}$ values have been determined, we calculate the denaturant concentration, C^*, at which $\Delta G = \Delta G^*$ by using:

$$C^* = C_{1/2} - \frac{\Delta G^*}{m_{1/2}} \qquad (17)$$

which is easily derived from eq 2. It is important to note that, since we have chosen the ΔG^* within the −8 to 8 kJ/mol range, application of eq 17 does **not** involve the linear extrapolation approximation, that is, we do use a linear equation but only within the range in which it describes adequately the experimental ΔG versus C data.

The above calculation (eq 17) is repeated for all the temperatures at which the solvent-denaturation profile has been characterized, to obtain several couples of C^*/T^* corresponding to the same ΔG^* value. These C^*/T^* values define a constant-ΔG line in the $C-T$ plane; the extrapolation of this line to $C = 0$ obviously yields the temperature, T_W, at which $\Delta G = \Delta G^*$ for zero denaturant concentration. In other words, this extrapolation determines a point of coordinates (ΔG^*,T_W) belonging to the protein stability curve at zero denaturant concentration. As shown in the Appendix, constant-ΔG lines are expected to show some curvature due (among other factors) to the large value of the denaturation heat capacity change. Therefore, the simplest way to perform the extrapolation is to fit the following second-order polynomial to the C^*/T^* data:

$$C^* = -\alpha(T^* - T_W) - \beta(T^* - T_W)^2 \qquad (18)$$

where the fitting parameters are α, β, and T_W. See the Appendix for a more detailed discussion on the origin of the extrapolating function and for a qualitative interpretation of the parameters α and β.

In fact, values of T_W may be obtained (as described above) for several values of ΔG^* within the −8 to 8 kJ/mol range. Therefore, the final outcome of the calculation will be the protein stability curve in water ($C = 0$) at high temperature, within the ΔG range −8 to 8 kJ/mol.

To the best of our knowledge, the procedure we have just described has not been employed previously in the literature. We name it the constant-ΔG extrapolation procedure and further dub it a nonlinear extrapolation procedure, not only because of the second-order polynomial used as extrapolating function (eq 18) but, mainly, because the procedure does **not** assume that the denaturant-concentration dependence of ΔG is linear over an extended range. (We emphasize again that the use of eq 17 in the constant-ΔG procedure is restricted to the narrow range in which the linear expression adequately describes the data.)

Application of the Constant-ΔG Extrapolation Procedure to the Urea-Induced Denaturation of Barnase. Experimental data reported in this work correspond to the guanidine-induced denaturation of HEW lysozyme. However, it appears convenient to illustrate first the application of the constant-ΔG procedure with the urea-induced denaturation of barnase, since a very careful study on this system has been recently published (Johnson & Fersht, 1995). Lysozyme denaturation will be taken up again in the next section of the present work.

Values of $C_{1/2}$ for urea-induced denaturation of barnase at several temperatures within the range 25−57 °C were taken from the $C-T$ equilibrium line reported in Figure 2 of Johnson and Fersht (1995). This equilibrium line was originally derived from DSC experiments performed in the presence of urea rather than from urea-denaturation profiles at constant temperature; this, however, is inmaterial for the illustration purposes of the present calculation. Note also that, since we intend to illustrate an extrapolation procedure, we use a comparatively narrow $C_{1/2}$ range (from 4.5 to 2 M), while data reported in Figure 2 of Johnson and Fersht (1995) extend, in fact, to zero urea concentration.

$m_{1/2}$ values for urea-induced denaturation of barnase were calculated from the data given in Table 3 of Matouschek et

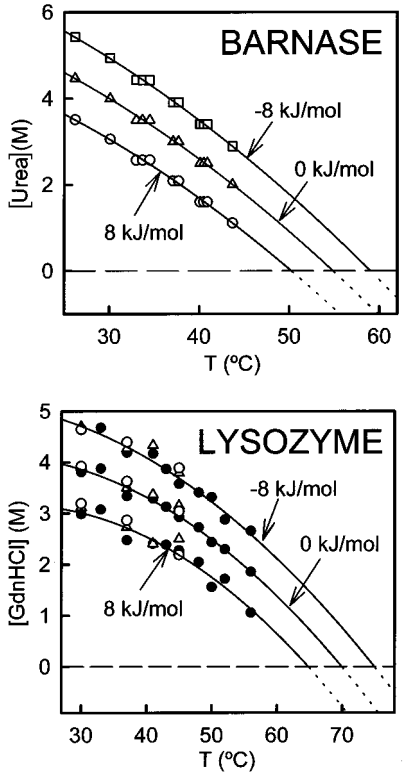

FIGURE 7: Constant-ΔG lines in the $C-T$ plane for the urea-induced denaturation of barnase (upper panel) and the guanidine-induced denaturation of lysozyme (lower panel). The continuous lines represent the best fits of eq 18 to the data. The numbers alongside the lines stand for the ΔG^* values corresponding to the lines. Values obtained from three different types of experimental data have been employed in the construction of the constant-ΔG lines for lysozyme: (●) equilibrium fluorescence intensity data (Figure 1 and eq 6), (△) unfolding assays (Figure 2 and eq 8), and (○) folding−unfolding kinetics (Figure 3 and eqs 9−11).

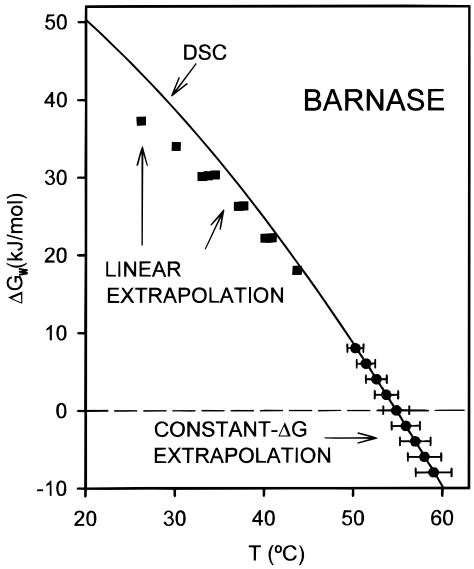

FIGURE 8: Temperature dependence of the Gibbs energy change for barnase denaturation at zero urea concentration. Values shown in this figure have been calculated from the results reported by Johnson and Fersht (1995); see text for details. Note that the constant-ΔG extrapolation procedure (see Figure 7 and eq 18) yields the T_W value for a given denaturation Gibbs energy; hence the standard errors (provided by the MLAB program) are associated with the temperature and are represented by horizontal bars in this figure.

al. (1995), which suggest that $m_{1/2}$ for urea-induced denaturation of barnase changes only slightly along the $C-T$ equilibrium line. We found that the $m_{1/2}$ values reported in this table could be adequately described by a linear equation in temperature: $m_{1/2} = 7.37 + 0.0377t$, where t is temperature in degrees Celsius and $m_{1/2}$ is given in kJ·mol^{-1}·M^{-1}. This linear equation was then used to calculate $m_{1/2}$ at the required temperature (and $C_{1/2}$) values.

Constant-ΔG lines were generated from the temperature, $C_{1/2}$, and $m_{1/2}$ values by using eq 17 and extrapolated to zero denaturant concentration by using eq 18 (see Figure 7A). Figure 8 displays the resulting ΔG_W versus temperature profile for zero denaturant concentration (and spanning the −8−8 kJ/mol ΔG range). We also show in Figure 8 the linear extrapolation estimates of the denaturation Gibbs energy in water (calculated from the $C_{1/2}$ and $m_{1/2}$ values by using eq 3) and the protein stability curve in water derived from the DSC data reported by Johnson and Fersht (1995). Note that the value for the linear extrapolation estimate of ΔG_W at 25 °C is 5.5 kJ/mol lower than that corresponding to the protein stability curve, a discrepancy already pointed out and carefully characterized by Johnson and Fersht (1995). On the other hand, the constant-ΔG method does not rely on a linear extrapolation and, in fact, yields ΔG_W values at denaturational temperatures in excellent agreement with the protein stability curve derived from DSC data (Figure 8).

Application of the Constant-ΔG Extrapolation Procedure to the Guanidine-Induced Denaturation of Lysozyme. Constant-ΔG lines in the $C-T$ plane for guanidine-induced denaturation of lysozyme are shown in Figure 7. Data points describing these lines span the 1−5 M guanidine concentration range approximately and were obtained (eq 17) from the previously calculated values of $m_{1/2}$ and $C_{1/2}$ at several temperatures (Figure 6). Note, however, that we have *not* used the DSC data at low guanidine concentration in the construction of these constant-ΔG lines.

Extrapolation of the constant-ΔG lines to zero denaturant concentration (see Figure 7) yields the ΔG_W versus temperature profile shown in Figure 9. Surprisingly, in this case the linear extrapolation estimates of ΔG_W and the values derived from the constant-ΔG method are both significantly lower than the DSC values and by approximately the same energy amount: about 15 kJ/mol. This agreement between the results obtained from the linear and the nonlinear extrapolations suggests that, at least to a first approximation, the guanidine-concentration dependence of ΔG is, in fact, linear over the extended range employed to construct the constant-ΔG lines (1−5 M, approximately) and that, therefore, significant deviations from this linear dependence (responsible for the 15 kJ/mol discrepancy) only appear at lower guanidine concentrations. This interpretation is consistent with the calculated values of $m_{1/2}$ (Figure 6B), *if we assume that the observed changes in $m_{1/2}$ are mainly due to a guanidine-concentration effect rather than to a temperature effect.* Thus (see Figure 6B), under this assumption, the $m_{1/2}$ value remains roughly constant within the 2−4 M guanidine-concentration range (implying a linear dependence of ΔG with C within that range), while it raises sharply below 1 M guanidine (approximately), implying that significant deviations from the linear dependence do occur but at low concentrations of the denaturant (that is, outside the concentration range employed in the constructions of the constant-ΔG lines of Figure 7).

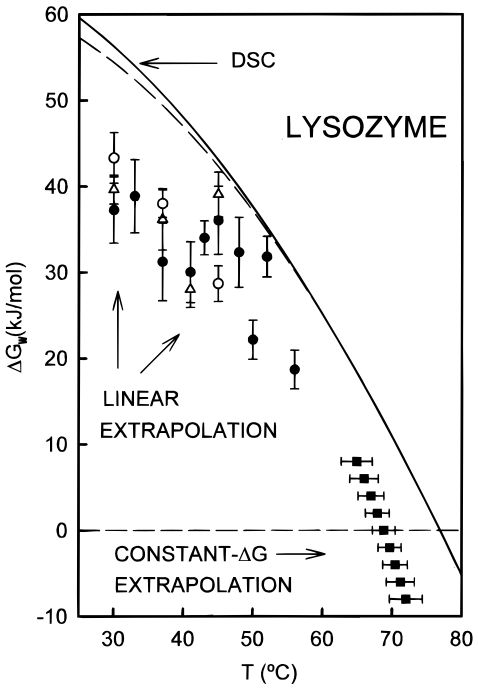

FIGURE 9: Temperature dependence of the Gibbs energy change for lysozyme denaturation at zero guanidine concentration. The meaning of the symbols for the linear extrapolation values and the lines representing the stability curves is the same as in Figure 5. Values obtained by using the constant-ΔG extrapolation procedure (Figure 7 and eq 18) are also included in this figure (■). Note the horizontal error bars (see legend to Figure 8).

Electrostatic Contributions to Lysozyme Stability and Their Relation with the Denaturation Gibbs Energy Values Determined from Guanidine-Denaturation Data. Guanidine hydrochloride, being a salt, is expected to significantly screen electric charges, even at concentrations about 1 M. Of course, charges are not screened to a large extent in a low-ionic-strength buffer at zero denaturant concentration. Therefore, it appears reasonable to assume that the electrostatic contribution to the denaturation Gibbs energy varies abruptly in the low-denaturant-concentration region, which could explain a strong deviation of the linear ΔG versus C dependence below 1 M, such as that described above for lysozyme. In fact, several authors have previously hinted or proposed that differences between the denaturation Gibbs energy values derived from urea and guanidine denaturation are related to electrostatic factors (Pace et al., 1990; Santoro & Bolen, 1992; Monera et al., 1994; Yao & Bolen, 1995; Smith & Scholtz, 1996). The idea is most clearly illustrated by the work of Monera et al. (1994) [see also Yu et al. (1996)]. These authors studied the urea- and guanidine-induced denaturation of four parallel, disulfide-bridged coiled-coils, which contained identical hydrophobic packing but different electrostatic interactions. Linear extrapolation values for ΔG_W derived from urea denaturation data were found to be widely different; on the other hand, those obtained from guanidine denaturation were very similar, suggesting that denaturing concentrations of guanidine supress an electrostatic contribution to ΔG.

It must be noted, however, that the term "electrostatic contribution" is often employed loosely in the literature (sometimes it appears to refer to charge−charge Coulombic interactions, sometimes to pH-dependent contributions to ΔG, sometimes to ionic-strength-dependent contributions, ...). In an attempt to avoid ambiguities, we will base our discussion on the approach recently employed by Yang and Honig (1993) [see also Yang et al. (1993), Honig et al. (1993), Yang and Honig (1994)]. Thus, following these authors, we write the denaturation Gibbs energy as: where $\Delta G^{neutral}$ contains

$$\Delta G = \Delta G^{neutral} + \Delta\Delta G^{ion} \qquad (19)$$

all Gibbs energy contributions to protein stability, except those involving electrostatic interactions of ionizable groups. $\Delta G^{neutral}$ is taken to be pH- and salt-independent. The pH-dependent term, $\Delta\Delta G^{ion}$, is given by:

$$\Delta\Delta G^{ion} = \Delta G^{ion}(U) - \Delta G^{ion}(N) \qquad (20)$$

where $\Delta G^{ion}(X)$ is the Gibbs energy of the state X (native or unfolded) taking as reference that state with all ionizable groups in their neutral forms.

$\Delta\Delta G^{ion}$ can be further separated into (a) contributions due to pairwise charge−charge interactions ($\Delta\Delta G^{q-q}$) and (b) contributions due to desolvation of charges (charge-dipole interactions are also included in this term) ($\Delta\Delta G^{desolv}$). Note that, from a continuum electrostatics point of view, the desolvation contribution is the consequence of the fact that, upon folding, charges are placed on the surface of a low-dielectric object, such as the native protein [see Yang and Honig (1993)]. Using this separation, eq 19 becomes

$$\Delta G = \Delta G^{neutral} + \Delta\Delta G^{desolv} + \Delta\Delta G^{q-q} \qquad (21)$$

Theoretical calculations based on continuum electrostatic models (Yang & Honig, 1993) support that, for HEW lysozyme, the pH-dependent term ($\Delta\Delta G^{ion}$ in eq 19) is always negative (that is, destabilizing) within the pH range 1−7. This is to be attributed to the desolvation contribution ($\Delta\Delta G^{desolv}$ in eq 21), which is negative and large in absolute value. In fact, the contribution due to charge−charge interactions ($\Delta\Delta G^{q-q}$ in eq 21) was found to be positive (that is, stabilizing) at neutral pH, reflecting the fact that positive and negative charges are distributed on the surface of the native protein so as to produce a net overall Coulombic attraction [that is, charges are, on average, surrounded by charges of the opposite sign; see Wada and Nakamura (1981), Matthew and Gurd (1986), Yang and Honig (1993)]. Nevertheless, $\Delta\Delta G^{q-q}$ becomes negative (destabilizing) at acidic pH, due to the neutralization of negative charges and the concomitant repulsion between the remaining positive ones.

A simple view about the guanidine effect on denaturation Gibbs energies would be as follows: At concentrations about 1 M, guanidine abolishes the electrostatic contribution from ionizable groups to ΔG, that is, the term $\Delta\Delta G^{ion}$ in eq 19 becomes negligible. $\Delta G^{neutral}$, on the other hand, could be expected to change gradually with guanidine concentration. As a result, the ΔG versus C dependence is linear (as a first approximation, at least) above 1 M guanidine (since, for $C > 1$ M, approximately, we expect $\Delta\Delta G^{ion} \approx 0$). Of course, at guanidine concentrations below 1 M, deviations from the linear dependence will occur, due to the abrupt change of $\Delta\Delta G^{ion}$ with salt concentration. Obviously, a linear extrapolation estimate of ΔG_W calculated from data obtained at guanidine concentrations above roughly 1 M guanidine will be approximately equal to the neutral contribution to ΔG at zero denaturant concentration:

$$\Delta G_W(\text{linear extrapolation}) \approx \Delta G_W^{\text{neutral}} \quad (22)$$

However, the above simple view is **not** consistent with our experimental results (Figure 9) when analyzed in the light of the theoretical calculations of Yang and Hoing (1993). These authors found that $\Delta\Delta G^{\text{ion}}$ for lysozyme in low-salt buffer is always negative, due to the desolvation contribution. Hence, the neutral contribution to ΔG_W must be higher than the actual value (which we assume to be given by the stability curve derived from DSC data). Therefore, if eq 22 were correct for lysozyme, the linear extrapolation estimates of ΔG_W would be larger than the actual values derived from DSC. However, the opposite situation is, in fact, observed in Figure 9.

An alternative, but equally simple, view could be that guanidine *gradually* alters the desolvation contribution ($\Delta\Delta G^{\text{desolv}}$ in eq 21), while *only* the contribution arising from charge−charge interactions ($\Delta\Delta G^{q-q}$ in eq 21) is abruptly eliminated (due to the screening effect) when going from zero to about 1 M guanidine concentration. In this case, the linear extrapolation estimate of ΔG_W would contain the neutral and desolvation contributions:

$$\Delta G_W(\text{linear extrapolation}) \approx \Delta G_W^{\text{neutral}} + \Delta\Delta G_W^{\text{desolv}} \quad (23)$$

and the difference between these linear extrapolation values and the actual ones derived from DSC would provide an estimate of the charge−charge contribution. If the results in Figure 9 are interpreted according to this view, then it is found that $\Delta\Delta G^{q-q}$ should be around 15 kJ/mol for lysozyme at zero denaturant concentration.

This second view is qualitatively consistent with the calculations of Yang and Honig (1993), since these authors found $\Delta\Delta G^{q-q}$ to be positive for lysozyme denaturation at pH 4.5 in low-salt medium. A quantitative test is not possible, however, due to uncertainties in the calculations. Thus, Yang and Honig (1993) reported two $\Delta\Delta G^{q-q}$ versus pH profiles for lysozyme, calculated employing two different structures for the protein: the triclinic crystal structure and a simulated structure derived from the former by using molecular dynamics. Qualitatively, these two profiles show the same trend: $\Delta\Delta G^{q-q}$ is positive at neutral pH and becomes negative at acidic pH. Quantitatively, they differ widely; for pH 4.5 the simulated structure gives $\Delta\Delta G^{q-q}$ about 30 kJ/mol, while the triclinic structure gives a value which is barely above zero. At least, we find encouraging that the value of about 15 kJ/mol we have estimated from our results (Figure 9) is right in the middle of the range defined by the two calculated values.

Comments on the Transition State for Lysozyme Unfolding at High Guanidine Concentration. Outside the transition zone, no curvature may be detected (within the scatter of the experimental data) in the unfolding branch of the Chevron plots shown in Figure 3. However, the slope of these plots (the kinetic $m_{N^{-}\ddagger}$ value) does change with temperature, as a visual inspection of Figure 3 clearly shows. The ratio between the kinetic *m* value and that corresponding to the unfolding equilibrium (that is, $m_{N^{-}\ddagger}/m_{1/2}$) is often used as an index for the degree of unfolding of the transition state, as compared with that of the denatured state, and, consequently, as a measure of the position of the transition state along the unfolding reaction coordinate (Tanford, 1970; Matouscheck & Fersht, 1993). Figure 10 shows a plot of this ratio versus

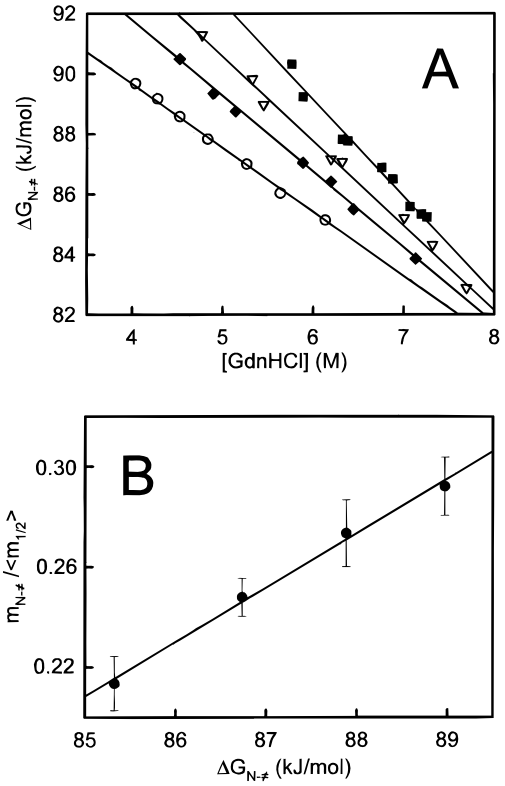

FIGURE 10: (A) Plots of activation Gibbs energy versus denaturant concentration for lysozyme unfolding at high guanidine concentrations. The data are calculated from the unfolding branches of the Chevron plots in Figure 3 by using transition-state theory with a transmission coefficient of unity and correspond to the following temperatures: (■) 18, (△) 30, (◆) 37, and (○) 45 °C. The lines represent the best fit of a general expression that describes both the temperature and the denaturant-concentration dependencies of the activation Gibbs energy (see text for details). (B) Hammond plot of kinetic $m_{N^{-}\ddagger}$ value (referred to the equilibrium $m_{1/2}$ value) versus activation Gibbs energy at 6 M guanidine. Since the error associated with the kinetic $m_{N^{-}\ddagger}$ is much smaller than that for the equilibrium $m_{1/2}$, the average value of the latter in the range 1.8−4 M ($\langle m_{1/2}\rangle$ = 10.5 kJ·mol^{-1}·M^{-1}) has been employed in the calculation.

the activation Gibbs energy for unfolding ($\Delta G_{N^{-}\ddagger}$) at $C = 6$ M, calculated from the unfolding rate constants by using transition-state theory. The plot is linear (within experimental uncertainty) and shows that the ratio $m_{N^{-}\ddagger}/m_{1/2}$ increases with the value of $\Delta G_{N^{-}\ddagger}$, which may be interpreted as an instance of *Hammond behavior*, that is, the transition-state position moves along the reaction coordinate, getting closer to the native state (lower $m_{N^{-}\ddagger}/m_{1/2}$ values) as the Gibbs energy difference between these two states decreases (lower $\Delta G_{N^{-}\ddagger}$ values). Evidence for Hammond behavior in protein folding has been previously reported for barnase and chymotrypsin inhibitor 2 (Matouscheck & Fersht, 1993; Matthews & Fersht, 1995; Matouscheck et al., 1995) with changes in activation Gibbs energy induced by mutation and temperature (evidence for anti-Hammond behavior has also been reported; Matthews & Fersht, 1995). In fact, the slope of our "Hammond plot" in Figure 10 ($\gamma = 2.2 \times 10^{-2}$ mol·kJ^{-1}, a measure of the sensitivity of the transition-state position to changes in activation Gibbs energy) is similar to the values published for barnase and chymotrypsin inhibitor 2.

An alternative view about the temperature-induced changes in $m_{N^{-}\ddagger}$ (which is not necessarily in conflict with the above interpretation in terms of Hammond behavior) arises from

the following linkage relationship:

$$\left(\frac{\partial m_{N-\ddagger}}{\partial T}\right)_C = \left(\frac{\partial \Delta S_{N-\ddagger}}{\partial C}\right)_T \quad (24)$$

which can be easily derived from the equality of the second cross-derivatives of the activation Gibbs energy. According to eq 24, the temperature effect on $m_{N-\ddagger}$ reflects a denaturant-concentration effect on the activation entropy ($\Delta S_{N-\ddagger}$).

It is straightforward to combine the linear $m_{N-\ddagger}$ versus $\Delta G_{N-\ddagger}$ dependence with the integrated Gibbs−Helmholtz equation to obtain an expression that describes both the temperature and denaturant-concentration dependencies of the unfolding activation Gibbs energy (result not shown). Fitting of this expression to the $\Delta G_{N-\ddagger}(T,C)$ data (see Figure 10) allows us to determine the transition-state energetics. Using this procedure, we find an activation enthalpy (at 30 °C and 6 M guanidine) of 129 ± 6 kJ/mol and an activation heat capacity of 0.9 ± 0.5 kJ·K^{-1}·mol^{-1}.

The value found for the activation heat capacity ($\Delta C_{p,N-\ddagger}$) is small compared with the heat capacity change for lysozyme denaturation [which is about 7−8 kJ·K^{-1}·mol^{-1} in water and appears to increase somewhat with guanidine concentration (Makhatadze & Privalov, 1992)], a result which qualitatively agrees with earlier work by Segawa and Sugihara (1984a). The interpretation of heat capacity changes is uncertain to some extent, since both positive contributions (from the exposure of apolar residues) and negative contributions (from the exposure of polar residues) are expected to be significant (Murphy & Gill, 1990, 1991; Makhatadze & Privalov, 1990, 1995; Spolar et al., 1992; Privalov & Makhatadze, 1992; Murphy et al., 1992; Sanchez-Ruiz, 1995). Nevertheless, the low values found for both the activation heat capacity and the ratio $m_{N-\ddagger}/m_{1/2}$ are consistent with a transition state in which comparatively little unfolding has taken place.

CONCLUDING REMARKS

To conclude, we wish to comment briefly on the two main points of the present work:

(1) We have proposed a new extrapolation method for the determination of denaturation Gibbs energies in the absence of denaturant from solvent-denaturation data (the constant-ΔG extrapolation procedure). The main features of this novel method, as compared with those of the linear extrapolation, are as follows.

(a) Both the constant-ΔG extrapolation and the linear extrapolation are model-independent procedures.

(b) The constant-ΔG extrapolation does **not** assume that the denaturant-concentration dependence of ΔG is linear over an extended concentration range, that is, *it is a nonlinear extrapolation procedure*.

(c) The constant-ΔG extrapolation requires several denaturation profiles (obtained at different temperatures), while a single denaturation profile (usually at 25 °C) suffices for the application of the linear extrapolation method.

(d) However, when applied at single temperature, the linear extrapolation method would only yield ΔG_W at that temperature, while the constant-ΔG extrapolation yields the protein stability curve (the ΔG_W versus T profile) within the −8 to 8 kJ/mol Gibbs energy range. This implies that, in principle, other thermodynamic quantities of interest may be evaluated. Thus, the denaturation enthalpy and entropy may be estimated as temperature derivatives of the stability curve: $\Delta H_W = -T^2(\partial[\Delta G_W/T]/\partial T)$ and $\Delta S_W = -(\partial \Delta G_W/\partial T)$; in favorable cases, even an estimate of the denaturational heat capacity change might be obtained if the curvature of the stability curve (Becktel & Schellman, 1987; Sanchez-Ruiz, 1995) is clearly apparent in the reconstructed "−8 to 8 kJ/mol" section. This suggests an interesting application of the constant-ΔG extrapolation: the characterization of protein folding energetics (denaturational changes in Gibbs energy, enthalpy, entropy, and, perhaps, heat capacity) in cases in which the irreversible character of the thermal denaturation precludes this characterization from DSC data (Sanchez-Ruiz, 1992, 1995) but in which solvent denaturation is found to be reversible.

(e) The linear extrapolation method has been often used to determine the effect of mutations on the denaturation Gibbs energy ($\Delta\Delta G$ values) at the reference temperature of 25 °C [see, for instance, Serrano et al. (1992)]. The constant-ΔG extrapolation may be used for the same task, but in this case, $\Delta\Delta G$ values will be necessarily calculated at a higher temperature. We do not consider this fact a drawback of the constant-ΔG extrapolation, since there appears to be no physical reason behind the traditional choice of 25 °C as reference temperature and protein engineering studies on the folding mechanism and stability could obviously employ a reference temperature different than 25 °C.

(f) The value of ΔG_W obtained by linear extrapolation is very sensitive to small errors in the $m_{1/2}$ value. For this reason, in protein engineering studies, $\Delta\Delta G$ values are sometimes calculated using the average of the $m_{1/2}$ values determined for the several protein variants (wild type and mutants) under study [see, for instance, Serrano et al. (1992)]. The values of ΔG_W determined by constant-ΔG extrapolation may also be sensitive to small errors in the parameters α and β (eq 18), but likewise, it should be possible to use average α and β values in the calculation of $\Delta\Delta G$ values, since these parameters appear to be related to overall energetic features of the protein (see Appendix) and are not expected to be significantly altered by nondisruptive mutations (unless, of course, the mutations have a strong effect on the possible residual structure of the denatured state; Shortle, 1993).

We have tested the constant-ΔG extrapolation procedure with experimental data for the urea-induced denaturation of barnase (Johnson & Fersht, 1995) and the guanidine-induced denaturation of HEW lysozyme (this work). Analysis of DSC experiments carried at different urea concentrations (Johnson & Fersht, 1995) supports that the urea-concentration dependence of ΔG for barnase denaturation is nonlinear over an extended [urea] range; in fact, a plot of ΔG versus [urea] shows a constant curvature (approximately), and consequently, the dependence may be adequately described by a second-order polynomial (Johnson & Fersht, 1995). The constant-ΔG extrapolation takes into account this "smooth" deviation from linearity and yields ΔG_W values at denaturational temperatures in excellent agreement with the protein stability curve derived from DSC experiments in the absence of denaturant (Figure 8). To the extent that the constant curvature observed by Johnson and Fersht (1995) in the ΔG versus [urea] plot is a general feature, this result (Figure 8) supports the applicability of the constant-ΔG extrapolation to the analysis of urea-induced denaturation.

On the other hand, our results would seem to suggest that the constant-ΔG extrapolation is likely to be less successful in the analysis of guanidine-induced denaturation. Thus, constant-ΔG extrapolation misses the abrupt deviation from linearity that appears to occur at low denaturant concentration in the guanidine-induced denaturation of lysozyme (*but so does linear extrapolation!* see Figure 9). However, an alternative and plausible point of view could be that, in the case of the guanidine-induced denaturation, both the constant-ΔG extrapolation and the linear extrapolation yield useful ΔG_W values, as long as it is recognized that a given salt-related contribution is not included in these calculated values [see eq 23 and point 2 below; see also Santoro and Bolen (1992), Yao and Bolen (1995)].

Overall, we believe that the first evaluation of the constant-ΔG extrapolation (presented in this paper) yields encouraging results. Of course, we do not claim at this stage that the constant-ΔG extrapolation is "superior" to the commonly employed linear extrapolation; these two methods cannot be compared on a fair basis, since linear extrapolation has been subject to a close scrutiny in recent years (see references quoted in the introduction of this work), while, obviously, extensive testing is not yet available for the novel constant-ΔG extrapolation. We do suggest, however, that the constant-ΔG extrapolation provides a practical, model-independent, and *nonlinear* alternative to the commonly employed linear extrapolation method.

(2) Our results on lysozyme denaturation suggest that the guanidine-concentration dependence of the denaturation Gibbs energy is, to a first approximation at least, linear over an extended concentration range but, also, that strong deviations from linearity may occur at low guanidine concentrations. We have tentatively attributed these deviations to the abrupt change of the contribution to ΔG that arises from pairwise, charge−charge electrostatic interactions. We point out that this contribution may be positive, negative, or close to zero, depending on the pH and the charge distribution on the surface of the native protein (Yang & Honig, 1993), which may help to understand why disparate effects have been found when studying protein denaturation at low guanidine concentration; thus, for instance, cases of negative deviation from linearity [see Figure 4 in Santoro and Bolen (1992)], positive deviation (see Figures 5 and 9 in the present work), and no significant deviation from linearity [see Discussion in Myers et al. (1995) and references quoted therein] have been reported. It is worth pointing out that if the contribution from charge−charge interactions is large and negative, then a stabilizing effect of moderate salt concentrations might be observed (as salt screens the destabilizing contribution). Interestingly, cases in which comparatively low guanidine concentrations stabilize native or molten globule states have been reported in recent literature (Mayr & Schmid, 1993; Hagihara et al., 1993), although these stabilizations may also be interpreted in terms of the binding of the guanidinium ion (Mayr & Schmid, 1993) or chloride ion (Hagihara et al., 1993) to the folded or partially folded states.

APPENDIX

Here, we will discuss in some detail the origin of the extrapolating function (eq 18) used in the constant-ΔG procedure. Equation 17 may be written as:

$$C^* = \frac{1}{m_{1/2}}(m_{1/2}\cdot C_{1/2} - \Delta G^*) \tag{25}$$

where $m_{1/2}\cdot C_{1/2}$ is the linear extrapolation estimate of ΔG_W at the temperature T^*. The difference between $m_{1/2}\cdot C_{1/2}$ and the actual ΔG_W value, although significant, is not likely to be very large. Therefore, a plot of $m_{1/2}\cdot C_{1/2}$ versus temperature will show a curvature roughly similar to that of the actual protein stability curve. Accordingly, the temperature dependence of $m_{1/2}\cdot C_{1/2}$ may be phenomenologically described by an equation of the Gibbs−Helmholtz form. The same is obviously true for the difference $m_{1/2}\cdot C_{1/2} - \Delta G^*$, since ΔG^* is a previously chosen constant value. Hence, the following equation appears to be a reasonable description of a constant-ΔG line in the $C-T$ plane:

$$C^* = \frac{1}{m_{1/2}}\left[\Delta H^{ap}\left(1 - \frac{T^*}{T_W}\right) + \Delta C_p^{ap}\left(T^* - T_W - T^* \ln\left(\frac{T^*}{T_W}\right)\right)\right] \tag{26}$$

where T_W is the temperature at which the difference $m_{1/2}\cdot C_{1/2} - \Delta G^*$ (and, consequently, C^*; see eq 25) becomes zero. Note that the enthalpy change and the heat capacity change in eq 26 have been labeled with a superscript "ap" to indicate that they are apparent values that phenomenologically describe the temperature dependence of the difference $m_{1/2}\cdot C_{1/2} - \Delta G^*$. Nevertheless, we do not expect them to be very different from the actual ΔH and ΔC_p values at the temperature T_W.

The temperature range of the constant-ΔG extrapolation (see Figure 7) is small compared with the absolute temperature values. Therefore, the following truncated Taylor expansion is an excellent approximation for the $T^* \ln(T^*/T_W)$ term in eq 26:

$$T^* \ln\left(\frac{T^*}{T_W}\right) \cong (T^* - T_W) + \frac{1}{2T_W}(T^* - T_W)^2 \tag{27}$$

Upon substitution of eq 27 into eq 26 we obtain

$$C^* = -\frac{\Delta H^{ap}}{T_W\cdot m_{1/2}}(T^* - T_W) - \frac{\Delta C_p^{ap}}{2T_W\cdot m_{1/2}}(T^* - T_W)^2 \tag{28}$$

If $m_{1/2}$ may be taken as a constant, then eq 28 would be identical with the extrapolating function proposed in the text (eq 18) and the parameters α and β in the latter equation would be given by:

$$\alpha = \frac{\Delta H^{ap}}{T_W\cdot m_{1/2}} \tag{29}$$

$$\beta = \frac{\Delta C_p^{ap}}{2T_W\cdot m_{1/2}} \tag{30}$$

However, even if $m_{1/2}$ changes gradually along the $C-T$ equilibrium line, we still expect eq 18 to be an adequate, phenomenological description of the constant-ΔG lines, although, in this case, the values of α and β would not be given by eqs 29 and 30. This is of little practical consequence since α and β are used as fitting parameters and, in any case, the apparent enthalpy and heat capacity changes

in eqs 29 and 30 (as well as the T_W value) are not known a priori. It is interesting, nevertheless, that rough estimates of α and β may be obtained from DSC data, together with a typical $m_{1/2}$ value. Thus, the denaturation temperature at zero denaturant concentration (T_m) may be used as an estimate of T_W and the actual ΔH and ΔC_p at T_m as estimates of the corresponding apparent values in eq 31. When this procedure is applied to lysozyme denaturation ($T_m = 350$ K, $\Delta H_m = 583$ kJ/mol, $\Delta C_p = 7.2$ kJ·K^{-1}·mol^{-1}, $\langle m_{1/2} \rangle = 10.5$ kJ·mol^{-1}·M^{-1}), eqs 29 and 30 give $\alpha = 0.16$ M/K and $\beta = 9.8 \times 10^{-4}$ M/K^2. These values are not very different from the actual ones obtained from the fitting of eq 18 to the constant-ΔG lines: α in the range 0.14−0.19 and β in the range $(15-19) \times 10^{-4}$.

Perhaps, the use of a second-order polynomial as an extrapolating function (eq 18 or 28) requires some additional comments. First, it must be noted that the use of the more complex eq 26 as an extrapolating function (with the ratios $\Delta H^{ap}/m_{1/2}$ and $\Delta C_p^{ap}/m_{1/2}$ as fitting parameters) yields essentially the same results as the second-order polynomial (results not shown); this result was to be expected, since eq 27 is an excellent approximation within a comparatively narrow temperature range and, consequently, eqs 26 and 28 (or 18) are equivalent for practical purposes in this case. Second, the use of higher-order polynomials does not lead to any improvement, and in particular, it does not eliminate the discrepancy observed between the (ΔG_W, T_W) values for lysozyme denaturation obtained by constant-ΔG extrapolation and the stability curve derived from DSC measurements (Figure 9). In fact, when we used a third-order polynomial in (T^*-T_W) to fit the constant-ΔG lines for barnase and lysozyme (Figure 7), we obtained meaningless T_W values with very large associated uncertainties (of the order of several hundred degrees in some cases; results not shown). Again, this result was to be expected; the experimental constant-ΔG lines (Figure 7) show a small curvature which is already well accounted for by a second-order polynomial. Therefore, the data do not contain information about higher-order terms in a polynomial expansion, and inclusion of these terms only leads to a very unreliable extrapolation. In general, we favor the use of a second-order polynomial, unless it is found that this simple function is unable to fit the experimental constant-ΔG lines; even in that case, however, caution must be exercised if using high-order polynomials as extrapolating functions, since these functions may show oscilating behavior outside the experimental value range.

NOTE ADDED IN PROOF

After this paper had been submitted for publication, Nicholson and Scholtz reported a careful study into the thermal and urea-induced denaturation of the histidine-containing phosphocarrier protein (HPr) from *Escherichia coli* (Nicholson & Scholtz, 1996). In this case, an accurate characterization of the denaturation energetics could be derived from noncalorimetric data, since cold denaturation was clearly evident in the thermal denaturation profiles. We have applied the constant-ΔG extrapolation procedure to the urea-induced denaturation of HPr by using the $C_{1/2}$ and $m_{1/2}$ values given in Table 1 of Nicholson and Scholtz (1996). The analysis of the reconstructed "−8 to 8 kJ/mol" section of the protein stability curve at zero urea concentration yields the following values for the denaturation temperature (T_g in the terminology employed by Nicholson and Scholtz) and the denaturation enthalpy and entropy at T_g: $T_g = 61.6$ °C, $\Delta H_g = 71.0$ kcal/mol, and $\Delta S_g = 212$ cal·K^{-1}·mol^{-1}. These values are in excellent agreement with those determined by Nicholson and Scholtz (Table 3 in these authors' paper) from the global analysis of the urea and thermal denaturation data. Since a slight curvature was detected in the "−8 to 8 kJ/mol" section of the stability curve, we could even derive an estimate of the denaturation heat capacity change (1.1 cal·K^{-1}·mol^{-1}), which is in acceptable agreement with the value given by Nicholson and Scholtz (1.4 cal·K^{-1}·mol^{-1}).

REFERENCES

Ahmad, F., Taneja, S., Yadav, S., & Haque, S. E. (1994) *J. Biochem. 115,* 322−327.

Alonso, D. O. V., & Dill, K. A. (1991) *Biochemistry 30,* 5974−5985.

Aune, K., & Tanford, C. (1969) *Biochemistry 8,* 4586−4590.

Bates, R. G. (1973) *Determination of pH. Theory and Practice,* 2nd ed., Wiley, New York.

Becktel, W. J., & Schellman, J. A. (1987) *Biopolymers 26,* 1859−1877.

Blinder, S. M. (1966) *J. Chem. Ed. 43,* 85−92.

Bolen, D. W., & Santoro, M. M. (1988) *Biochemistry 27,* 8069−8074.

Canfield, R. E. (1963) *J. Biol. Chem. 238,* 2691−2697.

Chen, B.-L., Baase, W. A., Nicholson, H., & Schellman, J. A. (1992) *Biochemistry 31,* 1464−1476.

Freire, E. (1995) *Methods Enzymol. 259,* 144−168.

Hagihara, Y., Aimoto, S., Fink, A. L., & Goto, Y. (1993) *J. Mol. Biol. 231,* 180−184.

Honig, B., Sharp, K., &Yang, A.-S. (1993) *J. Phys. Chem. 97,* 1101−1109.

Hu, C.-Q., Sturtevant, J. M., Thomson, J. A., Erickson, R. E., & Pace, C. N. (1992) *Biochemistry 31,* 4876−4882.

Johnson, M. J., & Fersht, A. R. (1995) *Biochemistry 34,* 6795−6804.

Makhatadze, G. I., & Privalov, P. I. (1990) *J. Mol. Biol. 213,* 375−384.

Makhatadze, G. I., & Privalov, P. L. (1992) *J. Mol. Biol. 226,* 491−505.

Makhatadze, G. I., & Privalov, P. L. (1993) *J. Mol. Biol. 232,* 639−659.

Makhatadze, G. I., & Privalov, P. L. (1995) *Adv. Protein Chem. 47,* 307−425.

Matouscheck, A., & Fersht, A. R. (1993) *Proc. Natl. Acad. Sci. U.S.A. 90,* 7814−7818.

Matouscheck, A., Otzen, D. E., Itzhaki, L. S., Jackson, S. E., & Fersht, A. R. (1995) *Biochemistry 34,* 13656−13662.

Matthew, J. B., & Gurd, F. R. (1986) *Methods Enzymol. 130,* 437−453.

Matthews, J. M., & Fersht, A. R. (1995) *Biochemistry 34,* 6805−6814.

Mayr, L. M., & Schmid, F. X. (1993) *Biochemistry 32,* 7994−7998.

Monera, O. D., Kay, C. M., & Hodges, R. S. (1994) *Protein Sci. 3,* 1984−1991.

Mücke, M., & Schmid, F. X. (1994) *Biochemistry 33,* 12930−12935.

Murphy, K. P., & Gill, S. J. (1990) *Thermochim. Acta 172,* 11−20.

Murphy, K. P., & Gill, S. J. (1991) *J. Mol. Biol. 222,* 699−709.

Murphy, K. P., Bakhuni, V., Xie, D., & Freire, E. (1992) *J. Mol. Biol. 227,* 293−306.

Myers, J. K., Pace, C. N., & Scholtz, J. M. (1995) *Protein Sci. 4,* 2138−2148.

Nicholson, E. M., & Scholtz, J. M. (1996) *Biochemistry 35,* 11369−11378.

Pace, C. N., & Vanderburg, K. E. (1979) *Biochemistry 18,* 288−292.

Pace, C. N., Shirley, B. A., & Thomson, J. A. (1989) in *Protein structure, a practical approach* (Creighton, T. E., Ed.) pp 311−330, IRL Press at Oxford University Press, Oxford.

Pace, C. N., Laurents, D. V., & Thomson, J. A. (1990) *Biochemistry 29,* 2564−2572.
Pfeil, W., & Privalov, P. L. (1976) *Biophys. Chem. 4,* 41−50.
Plaza del Pino, I. M., & Sanchez-Ruiz, J. M. (1995) *Biochemistry 34,* 8621−8630.
Privalov, P. L. (1979) *Adv. Protein Chem. 33,* 167−241.
Privalov, P. L. (1989) *Annu. Rev. Biophys. Biophys. Chem. 18,* 47−69.
Privalov, P. L., & Makhatadze, G. I. (1992) *J. Mol. Biol. 224,* 715−723.
Privalov, P. L., & Makhatadze, G. I. (1993) *J. Mol. Biol. 232,* 660−679.
Privalov, P. L., Plotnikov, V. V., & Filimonov, V. V. (1975) *J. Chem. Thermodyn. 7,* 41−47.
Sanchez-Ruiz, J. M. (1992) *Biophys. J. 61,* 921−935.
Sanchez-Ruiz, J. M. (1995) in *Subcellular Biochemistry, Volume 24: Proteins: Structure, Function and Engineering* (Biswas, B. B., & Roy, S., Eds.) pp 133−176, Plenum, New York.
Santoro, M. M., & Bolen, D. W. (1988) *Biochemistry 27,* 8063−8068.
Santoro, M. M., & Bolen, D. W. (1992) *Biochemistry 31,* 4901−4907.
Schellman, J. A. (1978) *Biopolymers 17,* 1305−1322.
Schellman, J. A. (1987) *Annu. Rev. Biophys. Chem. 16,* 115−137.
Schmid, F. X. (1992) in *Protein Folding* (Creighton, T. E., Ed.) pp 197−241, Freeman, New York.
Segawa, S.-I., & Sugihara, M. (1984a) *Biopolymers 23,* 2473−2488.
Segawa, S.-I., & Sugihara, M. (1984b) *Biopolymers 23,* 2489−2498.
Serrano, L., Kellis, J. T., Cann, P., Matouscheck, A., & Fersht, A. R. (1992) *J. Mol. Biol. 224,* 783−804.
Shortle, D. (1993) *Curr. Opin. Struct. Biol. 3,* 66−74.
Smith, J. S., & Scholtz, J. M. (1996) *Biochemistry* 35, 7292−7297.
Spolar, R. S., Livingstone, J. R., & Record, M. T. (1992) *Biochemistry 31,* 3947−3955.
Sturtevant, J. M. (1987) *Annu. Rev. Phys. Chem. 38,* 463−488.
Tanford, C. (1970) *Adv. Protein Chem. 24,* 1−95.
Wada, A., & Nakamura, H. (1981) *Nature 293,* 757−758.
Yang, A.-S., & Honig, B. (1993) *J. Mol. Biol. 231,* 459−474.
Yang, A.-S., & Honig, B. (1994) *J. Mol. Biol. 237,* 602−614.
Yang, A.-S., Gunner, M. R., Sampogna, R., Sharp, K., & Honig, B. (1993) *Proteins: Struct., Funct., Genet. 15,* 252−265.
Yao, M., & Bolen, D. W. (1995) *Biochemistry 34,* 3771−3781.
Yu, Y., Monera, O. D., Hodges, R. S., & Privalov, P. L. (1996) *Biophys. Chem. 59,* 299−314.

BI961836A